# Uncoupling High Light Responses from Singlet Oxygen Retrograde Signaling and Spatial-Temporal Systemic Acquired Acclimation[1][OPEN]

**Melanie Carmody, Peter A. Crisp, Stefano d'Alessandro, Diep Ganguly, Matthew Gordon, Michel Havaux, Verónica Albrecht-Borth, and Barry J. Pogson***

Australian Research Council Centre of Excellence in Plant Energy Biology, Research School of Biology, Australian National University, Canberra, Acton ACT 0200, Australia (M.C., P.C., D.G., M.G., V.A.-B., B.J.P.); Division of Plant Biology, Viikki Plant Science Center, Department of Biosciences, University of Helsinki, FI-00014 Helsinki, Finland (M.C.); and CEA, CNRS, Aix Marseille Université, UMR 7265 Biologie Végétale et Microbiologie Environnementales, Laboratoire d'Ecophysiologie Moléculaire des Plantes, F-13108 Saint-Paul-lez-Durance, France (S.A., M.H.)

**ORCID IDs: 0000-0001-5989-4801 (M.C.); 0000-0002-3655-0130 (P.A.C.); 0000-0002-0464-5549 (S.A.); 0000-0001-6746-0181 (D.G.); 0000-0001-6746-0181 (M.G.); 0000-0003-1869-2423 (B.P.).**

Distinct ROS signaling pathways initiated by singlet oxygen ($^1O_2$) or superoxide and hydrogen peroxide have been attributed to either cell death or acclimation, respectively. Recent studies have revealed that more complex antagonistic and synergistic relationships exist within and between these pathways. As specific chloroplastic ROS signals are difficult to study, rapid systemic signaling experiments using localized high light (HL) stress or ROS treatments were used in this study to uncouple signals required for direct HL and ROS perception and distal systemic acquired acclimation (SAA). A qPCR approach was chosen to determine local perception and distal signal reception. Analysis of a thylakoidal ascorbate peroxidase mutant (*tapx*), the $^1O_2$-retrograde signaling double mutant (*ex1/ex2*), and an apoplastic signaling double mutant (*rbohD/*F) revealed that tAPX and EXECUTER 1 are required for both HL and systemic acclimation stress perception. Apoplastic membrane-localized RBOHs were required for systemic spread of the signal but not for local signal induction in directly stressed tissues. Endogenous ROS treatments revealed a very strong systemic response induced by a localized 1 h induction of $^1O_2$ using the conditional *flu* mutant. A qPCR time course of $^1O_2$ induced systemic marker genes in directly and indirectly connected leaves revealed a direct vascular connection component of both immediate and longer term SAA signaling responses. These results reveal the importance of an EXECUTER-dependent $^1O_2$ retrograde signal for both local and long distance RBOH-dependent acclimation signaling that is distinct from other HL signaling pathways, and that direct vascular connections have a role in spatial-temporal SAA induction.

High light (HL)-mediated chloroplastic ROS retrograde signaling pathways derive from either (1) the conversion of molecular oxygen to singlet oxygen ($^1O_2$) through energy transfer reactions at photosystem II (PSII) or (2) the stepwise reduction of superoxide ($O\cdot$), hydrogen peroxide ($H_2O_2$), and hydroxyl radicals (HO) from electron transfer reactions, particularly those near photosystem I (PSI; Zhang et al., 2014). These ROS can initiate chloroplastic retrograde signals and have distinct transcriptional responses (op den Camp et al., 2003; Gadjev et al., 2006).

Until recently, chloroplastic $^1O_2$ has been considered the major ROS responsible for programmed cell death (PCD) signaling and cell damage, whereas $O\cdot/H_2O_2$ signaling from multiple compartments has been associated with HL acclimation (Triantaphylidès et al., 2008; Mullineaux and Baker, 2010). In recent years, studies have revealed how these ROS signals can in fact interact both synergistically and antagonistically and that ROS-derived signals generated in the chloroplast regulate both cell death and HL acclimation (Laloi et al., 2007; Baruah et al., 2009; Maruta et al., 2012; Ramel et al., 2012; Gordon et al., 2013). ROS signals additionally overlap with many hormone signaling pathways, revealing a richer complexity to their stress signaling functions (Lv et al., 2015; Xia et al., 2015; Shumbe et al., 2016). Chloroplastic $^1O_2$ and $O\cdot/H_2O_2$ are clearly capable of regulating both HL acclimation and PCD

[1] This project was supported by the Australian Research Council Centre of Excellence in Plant Energy Biology (CE140100008) and a YFP student travel scholarship to attend FEBS 2015, Croatia.

* Address correspondence to barry.pogson@anu.edu.au.

The author responsible for distribution of materials integral to the findings presented in this article in accordance with the policy described in the Instructions for Authors (www.plantphysiol.org) is: Barry J. Pogson (barry.pogson@anu.edu.au).

B.P. and V.A.-B. supervised the project; M.C., V.A.-B., B.P., and M.H. designed the experiments; M.C. performed and analyzed experiments with the exception of GC/MS performed and analyzed by S.A and additional qPCR and analyses performed by P.A.C. and D.G.; M.G. designed and established the LED HL array system; M.C., V.A.-B., and B.P. wrote the article with contributions from all authors.

[OPEN] Articles can be viewed without a subscription.

www.plantphysiol.org/cgi/doi/10.1104/pp.16.00404

 

signaling pathways; however, relatively little is known about the acclimation signaling pathways of $^1O_2$ (Ramel et al., 2012; Laloi and Havaux, 2015).

There is evidence that the cell death and acclimation outcomes of $^1O_2$ signaling eventuate in both EXECUTER (EX) dependent and independent signaling (Shumbe et al., 2016). Genetic screens for components of $^1O_2$ triggered cell death identified plastidic EX1 and EX2 by taking advantage of the conditional *flu(rescence)* mutant (Meskauskiene et al., 2001; Wagner et al., 2004; Lee et al., 2007). In the *flu* mutant, endogenous chloroplast-localized $^1O_2$ is produced from protochlorophyllide after a dark-light transition (Meskauskiene et al., 2001). The functions of the EX1 and EX2 proteins are unclear, yet mutant analysis indicates that disruption of the majority of $^1O_2$-responsive transcriptional changes occurs in the double mutant within the *flu* background (Lee et al., 2007), as well as wild-type Col-0 backgrounds (Kim et al., 2012). A second stress exposure with recovery in between required an EX1/EX2 retrograde signal that lead to acquired acclimation in exposed tissue (Lv et al., 2015), but what about rapid systemic signaling in this process? Another mutant used to demonstrate the acclimation regulation pathways of $^1O_2$ is the chlorophyll *b* mutant, *chlorina 1* (*ch1*), as it reflects the production of $^1O_2$ under HL at the site of PSII (Ramel et al., 2013). Studies of this mutant identified the $\beta$-carotene oxidation derivatives, $\beta$-cyclocitral and dihydroactinidiolide, that are produced very early in $^1O_2$-signaling (Ramel et al., 2012; Shumbe et al., 2014).

In addition to in situ responses to oxidative stress, the temporal-spatial nature of systemic signals has been shown to be important but is not well defined (Suzuki et al., 2013). While systemic movement of biotic signals from different organs of a plant are known to involve the vasculature, the spatial leaf connections in most abiotic stress studies are often not considered (Orians et al., 2000; Kiefer and Slusarenko, 2003; Heil and Ton, 2008; Carmody and Pogson, 2013). The transport of signaling molecules and hormones leaf-to-leaf is controlled by vascular architecture where connectivity between individual leaves is based on their phyllotactic arrangement in the rosette (Orians, 2005). Previous biotic studies have demonstrated how sampling between orthostichous (connected) and nonorthostichous (unconnected) leaves within plants can have a large effect on whether a particular study detects a response when leaf-to-leaf signal movement has a vascular component (Orians et al., 2000; Viswanathan and Thaler, 2004). If biotic signal movement is comparable to systemic abiotic signals, such as those generated under HL, then a study could find no distal response if the leaf shared no vascular connectivity or a very high response if directly connected.

Therefore, determining spatial distribution in terms of orthostichous connections between leaves of HL-induced signals such as systemic acquired acclimation (SAA; Karpinski et al., 1999; Rossel et al., 2007) would contribute to answering questions such as the direction of the signal, the requirement of the phloem source to sink vascular system, and whether other factors such as apoplastic and symplastic pathways or even volatile release may be involved. Separating ROS signals generated by the direct effects of stress from those involved in downstream acclimation and PCD signaling can be achieved through the use of localized stress experiments (Gordon et al., 2013). In this study, we investigated the behavior of long distance SAA signaling from two different points in the pathway: (1) the initiation of SAA through perception of HL and which retrograde signaling pathways are involved in SAA signal transduction from the chloroplast to the nucleus, and (2) investigation of what is required for the long-distance relay of the signal from leaf-to-leaf, including consideration of vascular connectivity.

## RESULTS

### ROS-Responsive Transcriptional Regulation of SAA

To obtain insight into the influence of different ROS responsive signals on the SAA transcriptional response, the SAA microarray published by Rossel et al., (2007) was compared with ROS-responsive gene sets compiled by Gadjev et al., (2006). Microarrays of SAA-induced genes were obtained from tissue taken from plants where a third of the rosette was treated with HL for 1 h (Rossel et al., 2007). The ROS-responsive gene sets were also chosen from analyses of the conditional *flu* mutant for $^1O_2$ specificity (op den Camp et al., 2003), KD-SOD (Rizhsky et al., 2003), and MV treatments for $O\cdot$ specificity (by D. Bartels from the AtGenExpress repository), as well as KO-APX1 (Davletova et al., 2005) and HL treatments of catalase-deficient mutants (Vanderauwera et al., 2005) for $H_2O_2$ specificity. Overall, around 25% of SAA genes were also ROS-responsive (89 genes, Fig. 1). Interestingly, the majority of these ROS-responsive genes responded to $^1O_2$ (Fig. 1; 16.48%), less than 1% were specific to $H_2O_2$ and/or $O\cdot$ and around 3% were general ROS response genes. A full list of ROS-responsive SAA genes, and list of $^1O_2$ responsive genes of known function are provided in Supplemental Table S1.

### Induction of SAA with Endogenous ROS

The microarray comparison indicated that $^1O_2$ signaling may be important for rapid SAA signaling in both local and distal leaves. As chloroplastic-derived $^1O_2$ is required for the HL response and due to the difficulties in separating $^1O_2$ from $H_2O_2$ generation during HL, endogenous ROS production strategies were employed to study whether specific ROS are required in SAA signaling.

Conditional *flu* mutants enabled the treatment of an individual leaf with a localized dark-to-light shift, illustrated in Figure 2, to induce an endogenous burst of $^1O_2$ in a noninvasive manner. Additionally, this

A

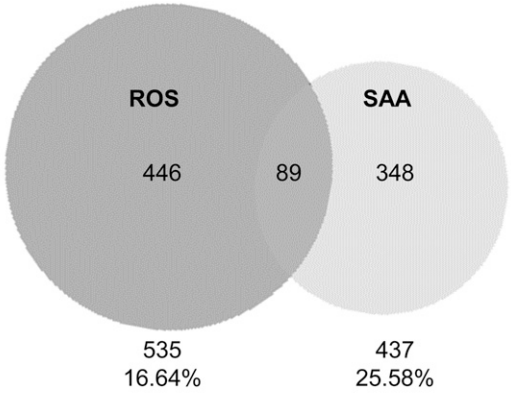


B

| ROS | Shared Transcripts | % |
|---|---|---|
| $^1O_2$ | 72 | 16.48 |
| $O_2^-$ | 1 | 0.23 |
| $H_2O_2$ | 3 | 0.69 |
| General Stress | 13 | 2.97 |

**Figure 1.** Comparison of SAA and ROS-responsive genes. A, Venn diagram of coexpressed transcripts between SAA microarrays from Rossel et al. (2007) and ROS responsive gene sets from Gadjev et al. (2006). B, The number and percentage of SAA and ROS-responsive genes coexpressed and their transcriptional responses to specific ROS ($^1O_2$, op den Camp et al., 2003; KD-SOD, Rizhsky et al., 2003; MV, D. Bartels, AtGenExpress; KO-APX1, Davletova et al., 2005; HL-treated catalase deficient mutanta, Vanderauwera et al., 2005).

treatment may induce a particularly specific chloroplastic $^1O_2$ signaling response as it can bypass PSII $^1O_2$ production induced under HL, avoiding additional cross-talk from other pathways (Mullineaux and Baker, 2010). *ELIP2*, monitored across all qPCR experiments in this study as a HL-inducible but distally unresponsive control, was not significantly induced by the endogenous $^1O_2$ produced in the *flu* background. The SAA marker gene *RRTF1* was significantly induced in both the treated leaf as well as upper and lower tissues (one-way ANOVA: $P = 0.043$). Interestingly, much higher induction of this gene was seen in lower distal tissue (Holm-Sidak post hoc test: $P = 0.009$) than in the dark-light shifted leaf (position 6) where the endogenous $^1O_2$ treatment was localized. This endogenous $^1O_2$ treatment method therefore resulted in a larger SAA distal response than under HL alone (Fig. 3). Transcripts of different ROS responsive genes were also monitored in the same tissues to demonstrate the specificity of the $^1O_2$ treatment (Fig. 2): *NodL* ($^1O_2$ and SAA), markers induced by rose bengal, *AAA-ATPase*, and *BAP1* ($^1O_2$; Baruah et al., 2009), and *FER1* induced by exogenous $H_2O_2$ and methyl viologen (MV; op den Camp et al., 2003). *AAA-ATPase*, a commonly used $^1O_2$ marker induced by rose bengal, is not responsive to HL and systemic signals reaching distal tissues in the SAA microarray (Supplemental Fig. S1; Rossel et al., 2007). *AAA-ATPase* is therefore a useful marker to compare the HL conditions of this study with others that have used much harsher conditions to study cell death signaling (Supplemental Fig. S1; Shao et al., 2013). Very high induction of the $^1O_2$ and SAA-responsive marker, *NodL*, was seen in treated and distal tissues (*NodL*, $P < 0.01$). Interestingly, *FER1* was slightly, but significantly, induced ($P < 0.05$) in distal and local tissues.

Chloroplast-derived $H_2O_2$ accumulation was investigated for its role in SAA as both ROS play roles in establishing cellular status (Chan et al., 2016). Stable *tAPX* overexpression (tAPX OE) and silenced (*tapx*) lines were compared to Col-0 for the potential contribution of compartment-specific chloroplastic $H_2O_2$ signals during SAA (Murgia et al., 2004; Yao and Greenberg, 2006; Laloi et al., 2007). Overexpression of *tAPX* should theoretically lead to reduced $H_2O_2$ accumulation in the chloroplast, whereas silenced *tAPX* lines may overaccumulate $H_2O_2$.

Given that tAPX is situated in the chloroplast and likely to be required early in the HL response, *ELIP2* induction was assessed in both OE and silenced lines to determine whether an adequate HL response was received in each plant in order for an SAA signal to be induced in distal tissue (Fig. 3). While significant induction of *ELIP2* was seen in HL-treated tissue in both lines, of the different tAPX germplasm, only the OE line had gene induction within a 100-fold order of magnitude (one-way ANOVA, $P = 0.007$; Fig. 3). The strong silenced line, *tapx*, was an order of magnitude less, although still significantly above LL (Holm-Sidak post hoc test: $P = 0.002$; Fig. 3A). The reduced *ELIP2* induction in *tapx* compared to tAPX OE was taken into account when interpreting whether this line had an impaired SAA or HL response.

Analysis of *ZAT10* activity in the OE and silenced lines showed that after 1 h of localized LED HL, the tAPX OE line gave a *ZAT10* induction profile similar to what would be expected in wild type (Fig. 3B). On the other hand, *tapx* had impaired *ZAT10* induction in treated and both distal tissues (Fig. 3A). *RRTF1* showed variable induction in HL and distal tissues of both transgenics. Additional ROS responsive markers were also monitored in these lines for comparison with other studies; however, most were not significantly induced in HL and most distal tissues (Supplemental Fig. S1). Of these, *AAA-ATPase* showed significant induction in distal, but not locally stressed, tissues of tAPX OE (Supplemental Fig. S1). *FER1* was not induced in either transgenic compared to a large induction in wild-type HL treated tissues and small but significant induction in distal tissues (Supplemental Fig. S1).

### Uncoupling HL and SAA Signals

The ROS-signaling mutants tested for impairment of HL and SAA signaling were the *EXECUTER* $^1O_2$

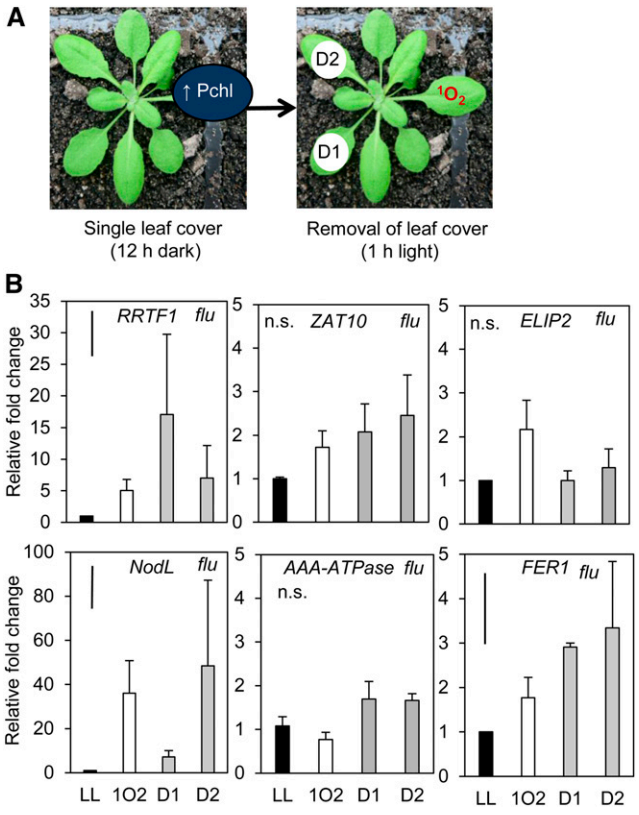


**Figure 2.** Analysis of SAA and ROS-responsive transcripts after localized endogenous chloroplastic $^1O_2$ generation within a single leaf. A, The dark-light shift treatment method of a single leaf using the conditional *flu* mutant. Leaf covers were applied to leaf position 6 for 12 h in order for protochlorophyllide (Pchl) to accumulate in the dark. Leaf covers were then removed for 1 h under growth light (120 $\mu$mol photons $m^{-2}$ $s^{-1}$) to generate localized endogenous $^1O_2$. Pchl, Protochlorophyllide. B, *RRTF1* (SAA marker), *ZAT10* (SAA marker), *ELIP2* (HL marker), *NodL* ($^1O_2$ responsive SAA marker), *AAA-ATPase* (SAA-independent $^1O_2$ marker), and *FER1* ($H_2O_2$ marker) transcript accumulation in treated and distal tissues of the *flu* mutant relative to untreated *flu* plants. LL, low light; $^1O_2$, endogenous $^1O_2$ treated leaf position 6; D1, lower distal leaf position 5; D2, upper distal leaf position 7. One-way ANOVAs were performed on each data set, post hoc Fisher's LSD results are displayed as a bar in the top left corner of each plot. n.s., Not significant. Error bars represent SE, $n = 3$.

signaling mutants *ex1*, *ex2*, and *ex1/ex2* in the Col-0 background, and the RESPIRATORY BURST OXIDASE HOMOLOG (RBOH) double mutant, *rbohD/F*, which is impaired in extracellular O· and $H_2O_2$ generation. The EXECUTER mutants were initially screened in the *flu* background for photobleaching development under continuous HL (Lee et al., 2007). In the Col-0 background, bleaching could also be detected after 4 d of relatively severe stress where plants transitioned from very low light conditions to moderate intensity halogen light at cold temperature (Kim et al., 2012). Because we were investigating rapid signaling events to different light conditions, it was necessary to assess whether photobleaching could occur under our HL conditions. Time point images were taken with the use of a Scanalyzer optimized to distinguish between photobleached and healthy leaf tissue (Supplemental Fig. S2). While bleached tissue was successfully distinguished from healthy green tissue, results indicated that there were no statistically significant differences in photobleaching development under continuous HL in vivo between the ROS mutants compared to wild type over 66 h (Supplemental Fig. S2). As no distinction could be made between mutants based on photobleaching within a few hours, the more sensitive qPCR assay was chosen for further analysis of rapid SAA signaling.

The SAA marker genes *ZAT10* and *RRTF1* were assayed in LL and HL (1500 $\mu$mol $m^{-2}$ $s^{-1}$) treated leaves (leaf position 6), as well as distal leaves five and seven. LL tissue sets of each genotype were initially compared relative to the equivalent LL wild-type tissue set in order to rule out basal up-regulation or down-regulation of *ZAT10* and *RRTF1* (Supplemental Fig. S3).

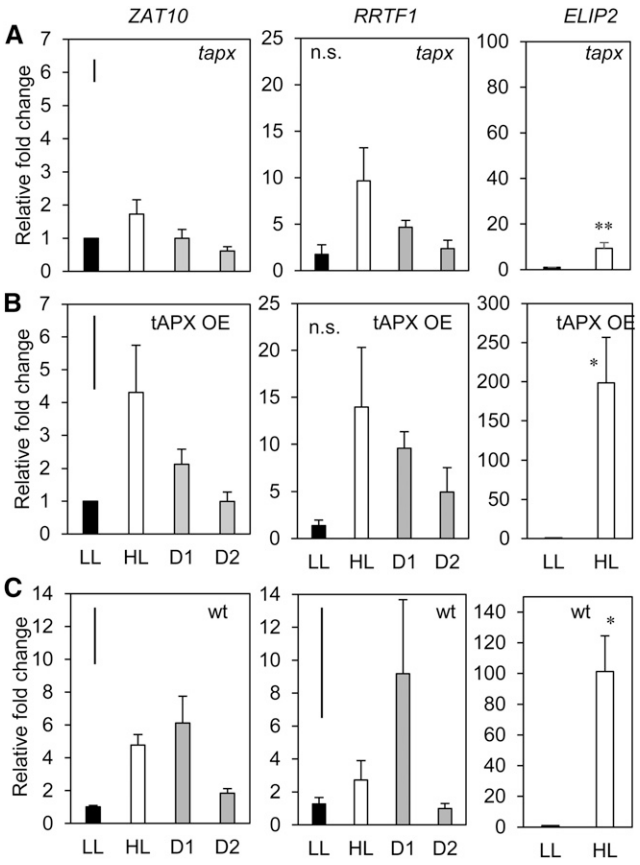


**Figure 3.** Endogenous manipulation of the chloroplastic ROS environment using stable silenced and overexpressing tAPX lines. Transcriptional analysis of *ZAT10, RRTF1* (SAA markers), and the *ELIP2* HL marker in *tapx 2/1* and the tAPX -14/2 overexpression lines compared to wild type (A) *tapx-2/1*, (B) tAPX-14/2, (C) wild type Col-0. LL, low light; HL, high light; D1, lower distal leaf position 5; D2, upper distal leaf position 7. One-way ANOVAs were performed on each *ZAT10* data set, post hoc Fisher's LSD results are displayed as a bar in the top left corner of each plot. *t* test were performed on *ELIP2* data sets. *$p < 0.05$ *$P < 0.005$. Error bars represent SE, $n = 3$.

One-way ANOVAs of mutant wild-type LL tissue sets were not significant, demonstrating that the basal LL response of each mutant was comparable to that of wild-type plants for these SAA marker genes (Supplemental Fig. S3).

*ZAT10* and *RRTF1* induction in HL and distal tissues from each mutant revealed various points of SAA impairment, as seen in Figure 4. The *ex1* data set showed no *ZAT10* or *RRTF1* induction of distal tissue compared to LL (Fig. 4). In *ex1*, *ZAT10* HL tissue was only induced 2-fold, however, was still significantly above LL (Holm-Sidak, $P = 0.004$), *RRTF1* had no significant differences across all tissues ($P = 0.076$). The *ex1/ex2* mutant was similarly impaired in distal *ZAT10* and *RRTF1* induction and additionally had no significant *ZAT10* or *RRTF1* induction in HL tissue (Fig. 4). The expression of *ZAT10* in upper distal tissue of the double mutant was significantly reduced (Holm-Sidak, $P = 0.006$), but no significant changes in RRTF1 were seen ($P = 0.397$). In contrast, SAA marker gene activity in *ex2* had similar fold changes to wild-type tissue, and the gene was significantly induced in all tissues relative to LL (*ZAT10* $P = 0.005$; *RRTF1* $P = 0.001$; Fig. 4). *The rbohD/F* mutant had a 3- to 4-fold induction of *ZAT10* and 20-fold induction of *RRTF1* in HL tissue compared to LL ($P = 0.001$ and $P = < 0.001$, respectively; Fig. 4) and low, yet significant, induction of *ZAT10* in both distal tissues (Fig. 4; *ZAT10* $P = 0.003$, D1; $P = 0.017$, D2). As with *ZAT10* gene induction, distal induction of *RRTF1* was low, however, in this case was not significant (Fig. 4). Statistical analyses of these data sets can be found in Supplemental Table S2A and S2B.

Overall, the SAA profile in HL and distal tissues followed a similar pattern for both SAA marker genes. While the SAA response in *ex2* was similar, if not more induced than in wild type, it is significant that *ex1* and *ex1/ex2* both lacked a distal response and had a greatly reduced HL response, particularly the double mutant. Interestingly, the *rbohD/F* double mutant was still responsive to HL but lacked a distal response.

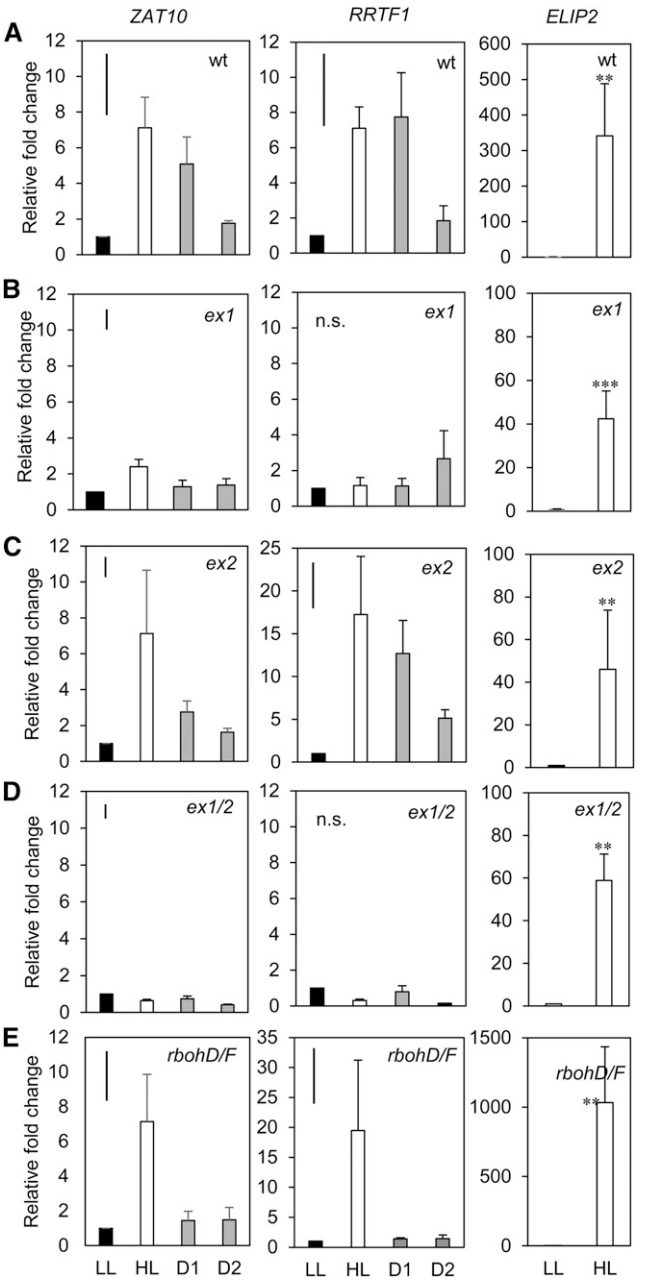


**Figure 4.** Transcriptional analysis of HL and SAA gene transcript responses in ROS signaling mutants. Transcriptional analysis of the *ZAT10*, *RRTF1* SAA marker and the *ELIP2* HL marker in ROS signaling mutant backgrounds (A) wild type, (B) *ex1*, (C) *ex2*, (D) *ex1/2*, (E) *rbohD/F*. LL, low light; HL, high light; D1, lower distal leaf position 5; D2, upper distal leaf position 7. One-way ANOVAs were performed on each data set, post hoc Fisher's LSD results are displayed as a bar in the top left corner of each plot. $^{**}p < 0.05$, $^{***}p < 0.005$, n.s., not significant. Error bars represent SE, $n$ = variable, see "Materials and Methods."

### Spatial Assessment of HL Defense and Acclimation Phenotypes

A number of analyses were performed to determine whether photoprotective pigment accumulation and photobleaching could be used as a visual marker for oxidative stress. Images were taken of phenotypic changes that occur over time under a 1000 $\mu$mol $m^{-2}$ $s^{-1}$ HL spot treatment in local and distal tissues. Figure 5 shows visual (A–C) and quantitative (D) investigation of the involvement of photoprotective mechanisms in SAA. A lightened area of the leaf occurs precisely within the area of the LED spotlight after 1 h HL exposure (Fig. 5A). Longer 15 h HL exposure results in similarly localized development of photobleaching and anthocyanin accumulation on the adaxial side of the leaf (Fig. 5, B and C).

Quantification of anthocyanin accumulation over time in control LL plants, as well as in distal and HL-treated tissues at 3, 6, and 15 h time points, can also be seen in Figure 5. Lightening of HL-treated tissues (possibly chloroplast movement), photobleaching, and

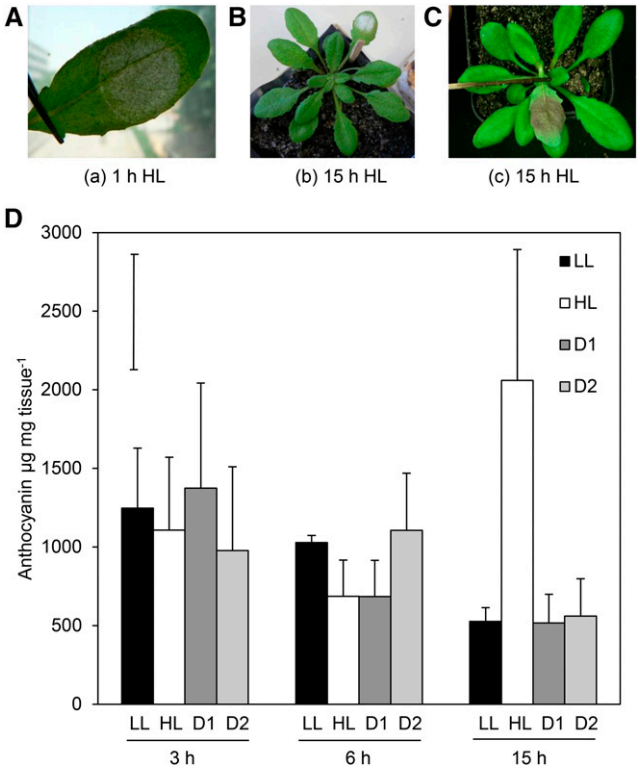


**Figure 5.** Visual HL stress marker and anthocyanin accumulation time course in local and distal tissue. A, Effect of 1 h HL on leaf tissue; B, photobleaching, 15 h HL; C, anthocyanin accumulation, 15 h HL; D, quantification of anthocyanin accumulation after 3, 6, and 15 h of continuous 1000 $\mu$mol photons $m^{-2}$ $s^{-1}$ HL, where black, LL control; white, HL-treated leaf at insertion 6; pattern, distal tissues at leaf positions 5 and 6, respectively. $n = 3$ samples of three pooled plants. Bar in top left corner represents Fischer's LSD post hoc test after one-way ANOVA (where $P = 0.006$). Error bars represent SD.

anthocyanin accumulation on the underside of the leaf is specifically induced under the LED HL spot. Both anthocyanin accumulation and oxidative stress bleaching is localized to the area of HL exposure, not to distal parts of the same leaf or distal leaves. A one-way ANOVA across all tissues and time points indicated that there were significant differences in the data ($P = 0.006$), specifically in HL-treated tissue after 15 h of exposure, which resulted in a 4-fold increase in anthocyanin content relative to LL (Holm-Sidak post-hoc test: $P < 0.001$). No differences in anthocyanin accumulation could be seen between LL and HL tissue after 1 h (Supplemental Fig. S4), 3 h, or 6 h (Fig. 5). It is clear from the above results that visual pigment accumulation is not an appropriate visual marker of SAA in distal tissue because anthocyanin accumulation is only detectable after at least 15 h of HL exposure under this treatment.

### Is There a Requirement of the Vasculature in SAA?

Plant phyllotaxis, not distance between leaves along the stem, determines vascular architecture and intensity of leaf interconnections (Esau, 1953). Previous experiments treated leaf position 6 and collected adjacent distal leaves 5 and 7 based on developmental age (Fig. 6A). However, the rapid transport of signaling molecules and hormones leaf-to-leaf is controlled by vascular architecture where connectivity between individual leaves is based on their phyllotactic arrangement in the rosette (Orians, 2005). Arabidopsis (*Arabidopsis thaliana*) has a helical phyllotaxis of 137.5° with three clockwise parastiches that connect every third leaf (n + 3) and five counterclockwise parastiches that connect every fifth leaf (n + 5; Evert and Esau, 2006). Leaf positions associated with vascular connections to leaf position 6 are illustrated in Figure 6B.

A new question was therefore asked: Is vasculature connectedness required for distal induction of SAA? To

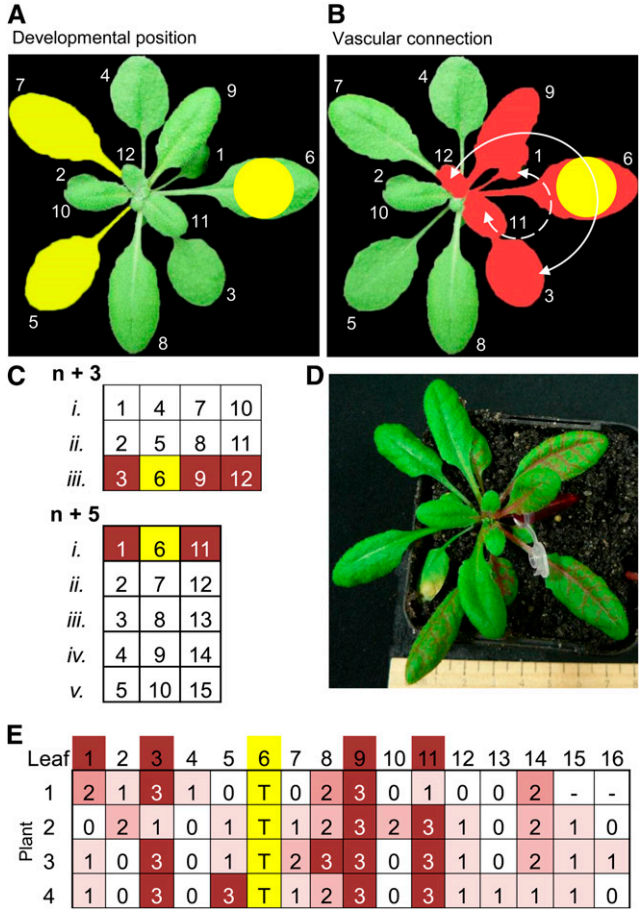


**Figure 6.** Rhodamine B petiole-feeding confirms immediate orthostichous connections between Arabidopsis leaves are capable of rapid signal movement. A, Developmental leaf positions. B, Vascular connections based on orthostichy. Leaf positions associated with vascular connections to leaf position 6 are indicated by white arrows, n + 3 orthostichie, and dotted white lines, n + 5 orthostichie. Rhodamine B was fed into the petiole of leaf 6, dye accumulation in specific leaves was scored after 2.5 h. C, Theoretical Arabidopsis orthostichies. D, Whole rosette 2.5 h after petiole dye feeding. E, Scoring matrix based on leaf position. Yellow, treated leaf; T, treated leaf; dye intensity scoring was from 0-3 where 0 related to no dye and 3 signified strong staining.

test this hypothesis, distal leaves at positions above and below the treated leaf were examined based on their developmental or orthostichous position within the rosette (Fig. 6 indicates different orthostichies, with direct leaf connections to leaf 6 highlighted). Both visual and quantitative methods were chosen to investigate this question, including the use of vascular dyes, visualization of ZAT10::LUC transgenics, and qPCR of the robust SAA marker genes, *ZAT10* and *RRTF1*.

### Confirmation of Arabidopsis Leaf Interconnections

Phyllotaxy is classically mapped with dyes (Orians et al., 2000). In Arabidopsis, orthostichous connections have been demonstrated over periods of 6–96 h after infiltration using isotope tracking and the herbicide, aminotriazole (Kiefer and Slusarenko, 2003). Dyes that progress more rapidly through the vasculature include Rhodamine B, which has previously been observed to move in real-time through tomato and tobacco vasculature (Orians et al., 2000). The petiole of leaf 6 was infiltrated with 0.25% Rhodamine B dye and dye accumulation recorded based on leaf position (Fig. 6). Predicted leaf connections are as indicated (Fig. 6). Interestingly, while orthostichous leaves accumulated the highest amount of dye, longitudinal connections with other leaves still occurred. More replicates of this experiment, along with petiole feeding through other leaves of the rosette, are provided in Supplemental Figure S5.

### Spatial and Temporal SAA Dynamics in Orthostichous Leaves

To investigate whether the vasculature is required for transmission of the SAA signal, tissues with direct vascular connections to leaf position 6 (leaves 3 and 9) were collected along with the standard distal leaf sampling (leaves 5 and 7). Additionally, a treatment of 5 min HL was included in order to assess the initial, rapid response of SAA compared to the standard 1 h HL treatment. A summary of statistical results can be found in Supplemental Table S3.

After the 5 min HL treatment, significant *ZAT10* induction was seen in HL-treated tissues compared to all other tissues (Holm-Sidak post hoc: $P < 0.001$; Fig. 7A). *ZAT10* expression in unconnected leaves was induced more than in connected leaves after 1 h HL (Fig. 7B); however, only gene expression in HL tissue was statistically significant relative to LL (one-way ANOVA: $P < 0.001$). Lower distal tissue (leaf 5) was significantly induced compared to both orthostichous leaves (Holm-Sidak post hoc: O1, $P = 0.033$; O2, $P = 0.022$). HL-specific *ZAT10*::LUC transgenics were also observed after these same treatment times; LUC localization can be seen in Figure 7 and Supplemental Figure S6. Observation of whole rosettes demonstrated that during the immediate 5 min HL response, LUC expression is concentrated in the vasculature of petiole tissue and midveins of most leaves (Fig. 7). More uniform spatial distribution of SAA by the 1 h time point can also be seen from the LUC imaging, where expression becomes localized within minor vein orders across most leaves in addition to the midveins (Figs. 7 and Supplemental Fig. S6).

The more responsive SAA marker gene, *RRTF1*, was also expressed in connected and unconnected distal tissues. The immediate *RRTF1* SAA response after 5 min HL was, however, significantly elevated in HL tissue (Holm-Sidak post hoc: $P < 0.001$) and in the lower orthostichous leaf tissue ($P = 0.002$; leaf 3, Fig. 8). After 30 min of HL treatment, average *RRTF1* expression was highly induced in HL-treated tissue as well as connected tissues (leaves 3 and 9). High variability in

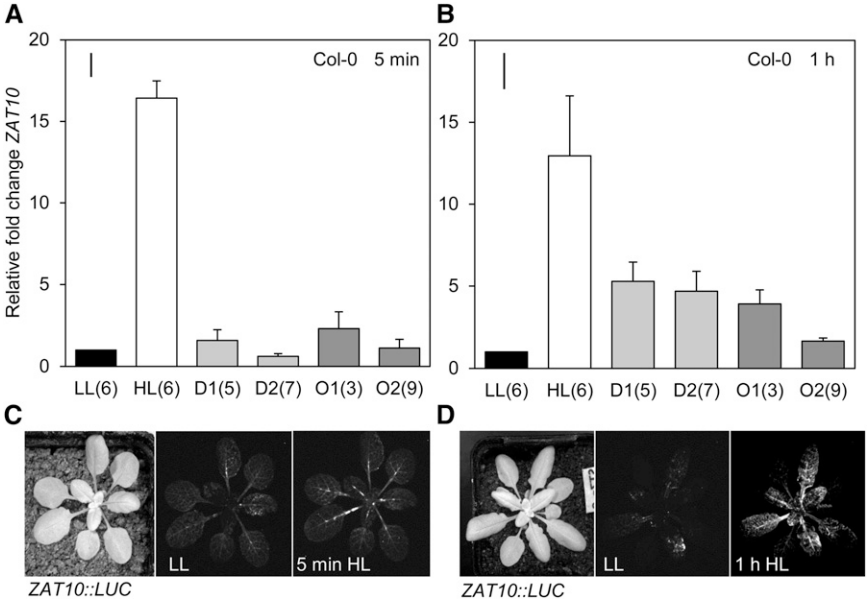


**Figure 7.** Spatial analysis of *ZAT10* expression after 5 min and 1 h localized HL. CCD imaging of ZAT10:LUC transgenics over the course of 1 h and the movement of signal from major vein orders to minor vein orders. LL, Low light; HL, high light; D1, lower distal leaf position 5; D2, upper distal leaf position 7. One-way ANOVAs were performed on each data set, post hoc Fisher's LSD results are displayed as a bar in the top left corner of each plot. Error bars represent SE, $n = 3$.

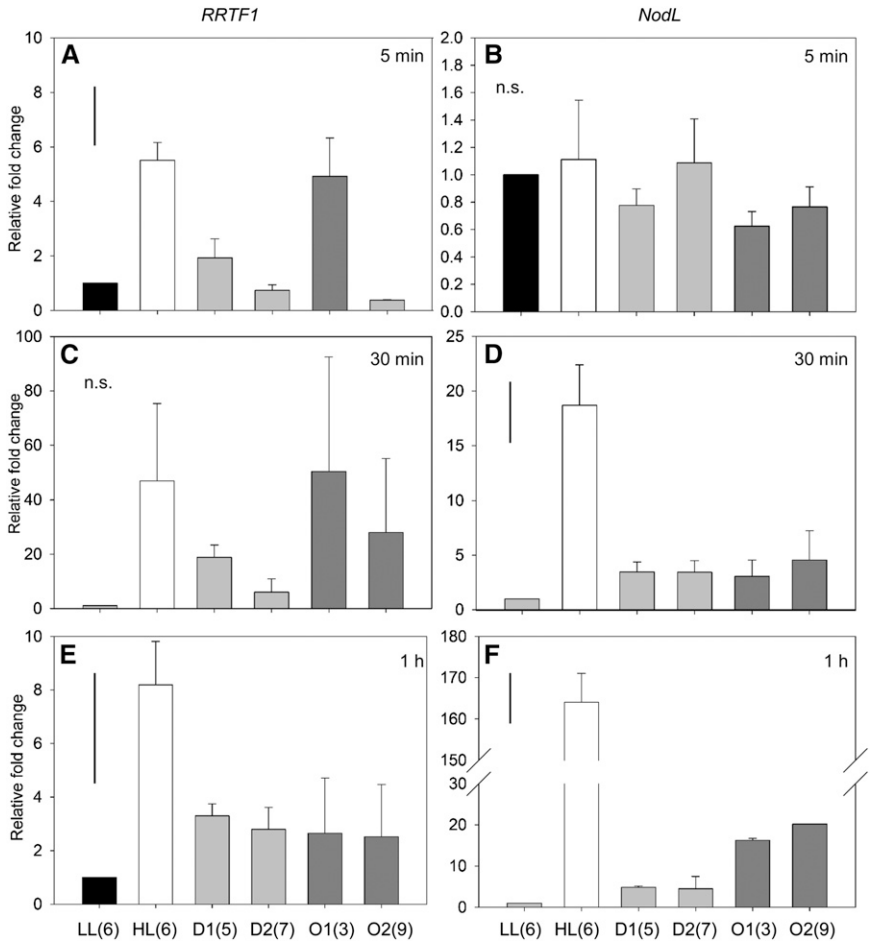


**Figure 8.** Time course of *RRTF1* and *NodL* expression in orthostichous tissue. qRT-PCR of *RRTF1* and *NodL* expression after HL treatments of (a) 5 min, (b) 30 min, and (c) 1 h. LL, leaf 6; HL, leaf 6; D1 and 2, distal leaves 5 and 7 respectively; O1 and 2, orthostichous leaves 3 and 9 respectively. Bar in top left represents Fischer's LSD after one-way ANOVA. $n = 3$.

results from this time point meant that these results were not significant (Fig. 8C). After 1 h, HL *RRTF1* expression was significantly induced in lower connected tissue (leaf 3, $P < 0.011$) and upper unconnected tissue (leaf 7, $P = 0.032$; Fig. 8). *RRTF1* distal gene expression was induced significantly above background and confirms the borderline significant trends seen by *ZAT10* activity, namely that orthostichous tissues may be required for the immediate SAA response between 5 and 30 min and that the signal appears to become more uniform (systemic) by the 1 h HL treatment time point.

An additional SAA and $^1O_2$-specific marker gene, *NodL*, was analyzed at these time points and showed a slightly different temporal response profile (Fig. 8). While this gene did not respond immediately to the 5 min HL treatment in any tissues (one-way ANOVA: $P = 0.718$), it was induced 20-fold after 30 min of HL exposure (Holm-Sidak post hoc: $P < 0.001$), and then increased proportional to the duration of HL exposure, as it was an order of magnitude higher after 1 h ($P < 0.001$). While *NodL* induction was still not significantly induced in any distal tissues after the 30 min HL-treatment, both upper and lower orthostichous tissues were significantly induced at the 1 h time point (leaf 3, $P = 0.013$; leaf 9, $P = 0.005$).

In summary, the orthostichous experiments showed that *ZAT10* and *RRTF1* distal expression appears to require the vasculature during the immediate 5 min response, and the response then becomes more uniform across the rosette by the 1 h time point. Localization of *ZAT10*::LUC luminescence shows how the signal is mostly concentrated within petioles and midveins at 5 min, and then begins to move into minor veins embedded in the mesophyll after 1 h HL. Conversely, the $^1O_2$-specific marker gene, *NodL*, was slower to respond to HL; however, the distal response remained specific to orthostichous tissues.

### SAA and β-Cyclocitral

Global expression comparison between SAA and β-cyclocitral transcriptional responses revealed the coexpression of 74 genes between these two data sets and that around 17% of SAA genes, including *ZAT12*, are also induced by β-cyclocitral (Fig. 9). Furthermore, many of these shared genes encode proteins expressed in the chloroplast, nucleus, plasma membrane, and plasmodesmata, together supporting both cell-to-cell and volatile signaling (Supplemental Table S4).

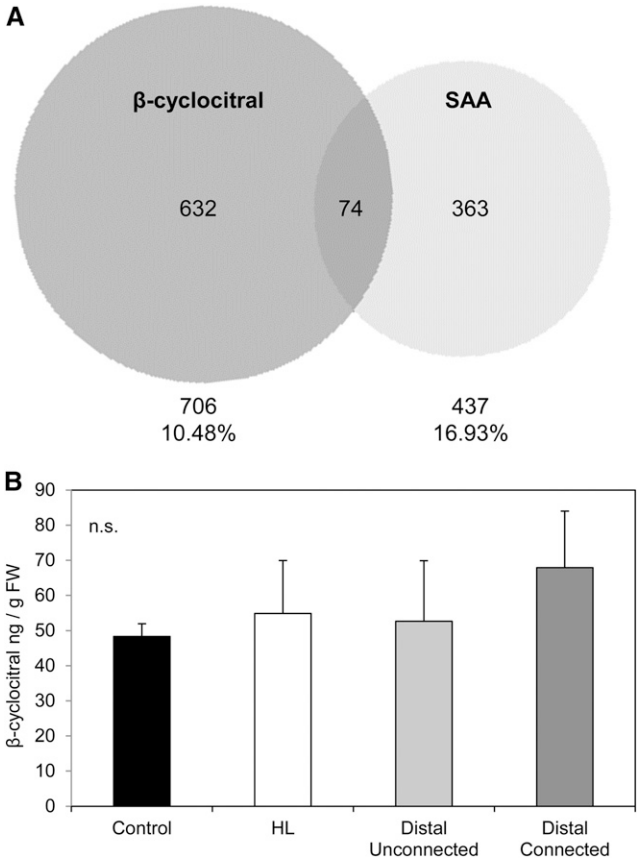


**Figure 9.** $\beta$-cyclocitral and SAA microarray comparisons and accumulation of compound under localized HL. A, Comparison of $\beta$-cyclocitral and SAA microarrays. Venn diagram of the $\beta$-cyclocitral microarray from Ramel et al., (2012) compared to the Rossel et al. (2007) SAA microarray. Total genes and percentages of shared genes are indicated under each data set. B, $\beta$-cyclocitral measurements from LL and LED-treated 1500 $\mu$mol photons $m^{-2}$ $s^{-1}$ HL leaf tissue. Relative changes of $\beta$-cyclocitral in local and distal tissues. Data are mean values of three independent measurements, SD = standard deviation.

GC/MS analysis was performed on local HL treated and distal leaves to measure the HL-induced signal $\beta$-cyclocitral concentrations (Fig. 9). The light treatment of 1500 $m^{-2}$ $s^{-1}$ at room temperature for 1 h, was not, however, sufficient to induce a significant accumulation of $\beta$-cyclocitral in HL-treated tissues compared to controls. Therefore, it was not possible to conclude whether induced $\beta$-cyclocitral is capable of inducing SAA; rather, HL of this intensity and duration is not sufficient to induce this $^1O_2$-induced volatile signal.

## DISCUSSION

This study reveals the importance of a rapid EXECUTER-dependent $^1O_2$ retrograde signal distinct from other HL signaling pathways required for both local and long distance SAA. That is, RBOHs are required for signaling to neighboring or distal tissues, but not in local tissues undergoing the direct effects of HL stress, and direct vascular connections are a component of spatial-temporal SAA induction. The requirement of $^1O_2$-signaling in SAA is unexpected given the large body of work produced over the last 15 years on the importance of $H_2O_2$, $Ca^{2+}$ and, more recently, intra- and extracellular RBOH-dependent cell-to-cell signaling (Kwak et al., 2003; Mittler et al., 2004; reviewed in Gilroy et al., 2016).

### The Importance of $^1O_2$ Signaling in Rapid SAA Initiation

Multiple retrograde signals are thought to be generated as a result of $^1O_2$ signaling (Oelze et al., 2012): as part of the EX1/EX2-dependent signaling pathway (Kim et al., 2008, 2012), through photo-oxidative damage caused by either direct cytotoxicity (Przybyla et al., 2008; Triantaphylidès et al., 2008; Oelze et al., 2012) or oxidized by-products of lipids and carotenoids (Ramel et al., 2012; Chan et al., 2016; Havaux, 2014). Transcriptional studies of ROS-specific transcripts in Arabidopsis reveal complex patterns of ROS-responsive transcripts under abiotic stress conditions (Baruah et al., 2009). Other mutant backgrounds have been reported recently where endogenous $^1O_2$ generation closer to where it is produced during HL stress is possible. This particular ROS is more pronounced under HL in the chlorophyll *b*-less light-sensitive mutant of Arabidopsis, *chlorina1*, *vte npq1* (Havaux et al., 2006, Havaux et al., 2007; Ramel et al., 2013) and *npq1 lut2,* the latter two missing key carotenoid components required in the HL response (Triantaphylidès et al., 2008, Alboresi et al., 2011). Collectively, these results indicate that there are multiple $^1O_2$-specific signaling pathways that could be involved in long-distance signaling in addition to results presented here. However, many of these are yet to be characterized let alone assessed for their involvement in SAA.

Results from this study demonstrate that $^1O_2$-signaling plays a major role during rapid SAA signal transduction. Twenty-five percent of rapid SAA genes respond to ROS; 70% of which can be induced by $^1O_2$ (Fig. 1). Several other studies have also indicated that the majority of ROS-responsive genes induced during stress responses are $^1O_2$-responsive in directly stressed tissues, although they did not look at systemic responses (Gadjev et al., 2006; Baruah et al., 2009; Laloi and Havaux, 2015). Additionally, the choice of the conditional *flu* mutant in this study enabled systemic analysis to be performed where endogenous stress signals were spatially uncoupled from tissues receiving the systemic signal. For example, systemic induction of one SAA marker gene, *RRTF1*, after a localized dark-light shift of a single leaf, indicated that $^1O_2$ signals can induce SAA from within the chloroplast (Fig. 2). Evidence of localized $^1O_2$ signal induction in *flu* from these treatments is also shown through the high induction of the $^1O_2$-specific and SAA marker gene, *NodL*, while only a small but significant induction of the $H_2O_2$ marker *FER1* was found to occur in locally stressed tissue (Fig. 2).

Intriguingly, the general stress and SAA marker, *ZAT10*, was not significantly induced in the *flu* background (Fig. 2). This indicates that some SAA genes ordinarily induced under HL are not initiated by *flu* $^1O_2$. One explanation for this is that *flu* $^1O_2$ signals are thought to be uncoupled from HL responses and have previously been shown to have an immediate cytotoxic effect on chloroplast membrane integrity, which is absent when $^1O_2$ is produced as a result of HL at PSII in Col-0 (Lee et al., 2007; Mullineaux and Baker, 2010; Kim et al., 2012). A commonly used $^1O_2$ stress marker, *AAA-ATPase*, was similarly absent in these conditions as well as in HL treated wild-type tissues under the conditions used herein, and in other studies using similar light regimes (Rossel et al., 2007; Shao et al., 2013). Similarly, *FER1* was not induced in local tissue; however, there was a small but significant induction in distal tissues in contrast to wild-type HL-treated tissue where this gene was strongly induced (Fig. 2).

The importance of $^1O_2$-signaling produced in the Col-0 background as a response to HL was also shown here to be required for SAA induction as both *ex1* and *ex1/ex2* in the wild-type Col-0 background were impaired or disrupted in the local HL-stressed leaf, respectively (Fig. 4). SAA marker genes measured in these mutants undergoing localized HL treatments responded in a similar way to the large scale $^1O_2$-regulated transcriptional responses documented in previous studies (Lee et al., 2007; Kim et al., 2012). For example, distal transcriptional responses were similarly enhanced in *ex2*, impaired in *ex1*, and almost completely disrupted in *ex1/2* across all studies. It is important to note that in this study the HL response was not impaired in the EXECUTER mutants, as indicated by the *ELIP2* marker (Fig. 4), and this suggests that initiation of the SAA signal, rather than the HL response, is EXECUTER-dependent.

### Uncoupling HL Defense Signals from Acclimation: Photoreceptor Pathways Are Distinct from SAA

Downstream from rapid HL and SAA perception in local HL stressed tissue, photoreceptor and photoprotection related pathways are demonstrated to be independent of the rapid SAA signaling pathway due to their absence in distal tissues. Images of HL defense phenotypes are presented in Figure 5, and these can be compared with the specific *ELIP2* induction in locally HL-stressed tissues (Figs. 2, 3, and 4). Visual phenotypes presented in Figure 5 demonstrate how photoprotective changes, such as photobleaching, and anthocyanin accumulation were localized exclusively within the region of the LED HL-treated spot. This simultaneously demonstrates the specificity of the HL treatment to the treated leaf. Differences between HL defense pathways and SAA are particularly evident in regards to the known relationships between *APX2*, *ELIP2*, and anthocyanin accumulation. Absence of photoprotective activity, as well as the general lack of *ELIP2* in distal tissues, indicates that other long-term acclimation pathways associated with this gene may also be independent of the SAA signal. Alternatively, this may indicate that SAA is a priming response and acclimation does not occur until the distal tissues are actually exposed to HL (Gordon et al., 2013). Although not directly systemic, long term studies of $^1O_2$ priming to a second stress exposure with recovery in between indicate how there is a loss of an acclimation effect in the *ex1/2* background (Lv et al., 2015), while a moderate light stress "priming" treatment suggested that $^1O_2$-signaling may confer long-term stress acclimation not just to a second more severe high light stress, but also induce cross-tolerance against a virulent *Pseudomonas syringae* strain (Zhang et al., 2014). These recent studies reinforce the results presented here in that rapid SAA initiation requires chloroplastic $^1O_2$-signaling and suggest that these rapid signals lead to longer term acclimation effects.

Many previous systemic studies have used the argument that the involvement of *APX2* in both HL and $H_2O_2$ signaling processes suggests crosstalk between these two pathways (Cheng et al., 2013). In contrast, the evidence that *APX2* may not be induced under HL-alone (Jung et al., 2013) indicate a level of complexity in the regulation of this gene. Likewise, there is a strong indication of how $^1O_2$-responsive genes and initiation of SAA may be independent of HL and even $H_2O_2$ initiation pathways, as well as how $^1O_2$ could result in a much earlier response. Future studies should focus on assigning a temporal and spatial component toward further uncoupling the interplay of different ROS-mediated pathways.

### The Antagonistic Relationship between $^1O_2$ and $H_2O_2$

The uncoupled *ZAT10* and *RRTF1* SAA responses in the dark-light shifted *flu* background suggest that different retrograde signals can initiate SAA and relay a particular signal to distal tissues, indicating that $^1O_2$-induced SAA is associated with downstream acclimation signaling. Distal marker gene induction in *flu* appeared to result in both $^1O_2$ and $H_2O_2$ responses, as *NodL* and *FER1* ROS-responsive markers were in some cases induced more than in treated tissue (Fig. 2). Localized stress application allows physical uncoupling of localized HL-defense and SAA signals (illustrated in Figs. 5 and 6). These uncoupled HL defense and SAA retrograde signals are shown in Figure 4 through simultaneous observation of the early HL response gene, *ELIP2*, and SAA genes, particularly *RRTF1*. These were assayed using qPCR in wild type as well as in *tapx* (lacking the thylakoid $H_2O_2$ scavenger) and *ex1/2* (disrupted in $^1O_2$-signaling). A model of the response of these genes in each of the different mutant backgrounds can be seen in Figure 10. While both HL and SAA genes were induced in wild type and SAA gene induction was blocked in *ex1/2* (Fig. 4); both SAA and HL gene inductions were blocked or downregulated in the *tapx*

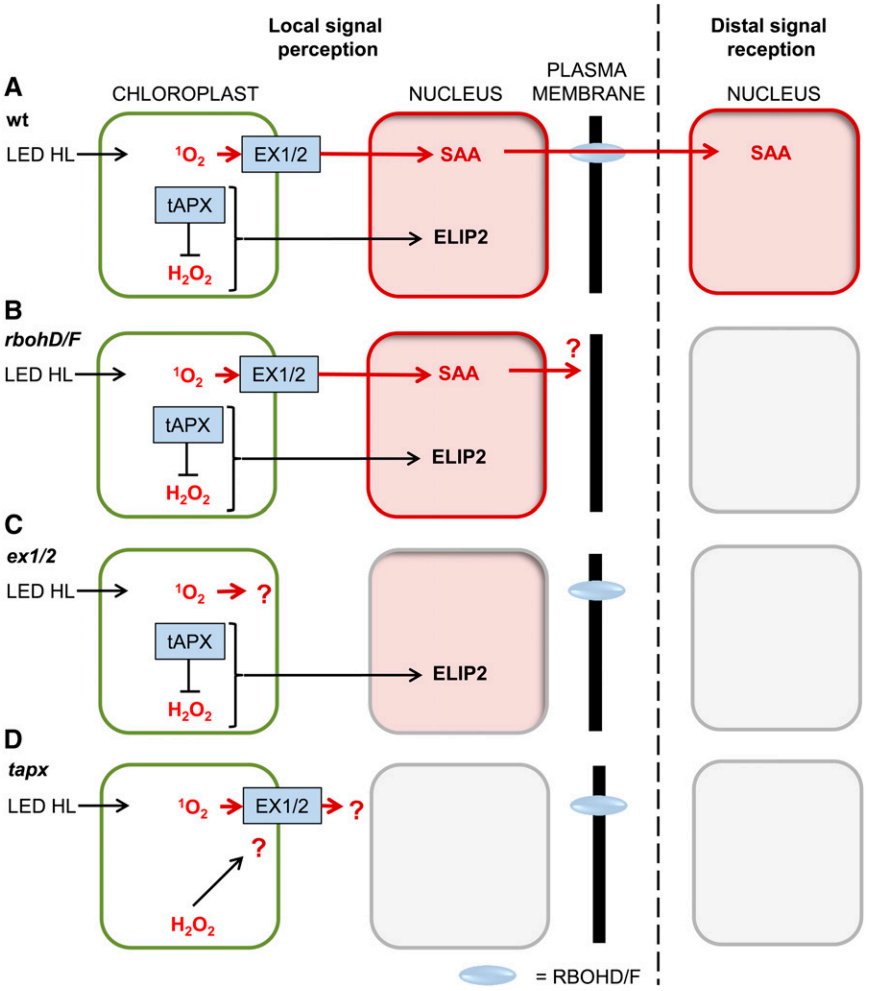


**Figure 10.** Model of antagonistic relationship between $^1O_2$ and $H_2O_2$ retrograde signaling pathways. Nuclear induction of SAA (*ZAT10* and/or *RRTF1*) and HL-response (*ELIP2*) genes under LED HL in local tissue stress perception and distal signal reception in (A) wild type, (B) *rbohD/F*, (C) *ex1/2*, and (D) *tapx* backgrounds.

background (Fig. 3). This suggests that elevated $H_2O_2$ in the absence of tAPX interferes either directly or indirectly with $^1O_2$ retrograde signaling. It therefore seems likely that *tAPX* is required for both the HL response and early SAA initiation events in Arabidopsis. A summary of these ROS results (Fig. 10) indicates how treatments or mutant backgrounds where $^1O_2$ levels were elevated, similarly induced SAA; while a decrease in this ROS species resulted in lack of local and distal SAA induction. In contrast, chloroplast-derived $H_2O_2$ resulted in the opposite effect in which an increase in this ROS meant that there was no SAA induction, and reduction resulted in a normal SAA signal.

It should be noted that the constitutive tAPX-OE and *tapx* lines do not necessarily reflect the increased or decreased $H_2O_2$ scavenging environments hypothesized, respectively. That is, conflicting results were earlier reported in these lines under various stress treatments (Laloi et al., 2007, Kangasjärvi et al., 2008, Maruta et al., 2010). This led to the study of inducible tAPX RNAi lines (Maruta et al., 2012), and one consensus was the constitutive tAPX overexpressing lines behaved very similarly to wild type and did not appear to have an effect, whereas the nonresponsiveness of marker genes to HL stress in *tapx* could indicate preacclimation to stress in this genetic background, compensated for by other scavenging systems. More direct assessment of the effects of tAPX-overexpressing and silenced lines would have to be performed in inducible lines to avoid the developmental acclimation effect in the stable backgrounds.

### Apoplastic $H_2O_2$ Is Required for the Distal SAA Response, but Not in Local Stressed Tissue

Analysis of the apoplastic $H_2O_2$ producing *rbohD/F* mutant confirmed that $H_2O_2$ is indeed necessary for distal acclimation of tissues to HL, but not in locally stressed tissue (Fig. 4). Induction of SAA marker genes in HL-treated tissues, but not distal tissues, may appear controversial in light of previous studies demonstrating the requirement of RBOHD for systemic cell-to-cell signaling along a floral bolt (Miller et al., 2009). However, this study not only sampled specific leaves within the vegetative rosette to track the signal from leaf-to-leaf, but also sampled HL-treated tissue exclusively from the LED spot, the boundary of which was visible

after the treatment as shown in Figure 5. RBOHD-dependent signaling is central to the "ROS wave" theory of rapid cell autonomous signal movement. These signals have been demonstrated to travel much more quickly than the SAA signals described here, most likely as a result of the additional electrochemical propagation of the signal (Karpinski and Szechynska-Hebda, 2010; Mittler et al., 2011; Gilroy et al., 2014; Mittler and Blumwald, 2015; Gilroy et al., 2016).

An interesting perspective on *APX2*, *ZAT10*, and apoplastic $H_2O_2$ is that they are all localized to bundle sheath cells (BSCs) or the adjacent apoplastic spaces that surround the vasculature of stressed tissue (Fryer et al., 2003; Galvez-Valdivieso et al., 2009). This could mean that $H_2O_2$-mediated control of *APX2* expression in bundle sheath cells is fundamentally different from that in other leaf tissues (Bechtold et al., 2008). In fact, recent work using differential photosynthetic changes to different chemical treatments demonstrates ABA, *APX2*, and $H_2O_2$ responses are distinct to BSCs compared to mesophyll (Suzuki et al., 2013; Gorecka et al., 2014). In *Oryza sativa*, altering NADPH/$NADP^+$ levels through $C_4$-like photosynthesis in BSCs promoted HL stress responses specific to the midvein (Shen et al., 2015). While BSC chloroplasts may specifically sense environmental conditions and relay these directly to the phloem to signal to distal tissues, this still does not explain the problem of signal specificity. A final hypothesis for retaining stress specificity as well as the common apoplastic $H_2O_2$ BSC vascular response model is that there may be an external volatile SAA signal as well as a more general stress response relayed through the vasculature.

#### Is the Vasculature Required for SAA?

In this study, the theory that plant phyllotaxis, not distance between leaves along the stem, determines vascular architecture was explored. The intensity of rhodamine B dye in orthostichous (connected) leaves of the Arabidopsis rosette scored after 2.5 h petiole feeding (Fig. 7) was used to investigate the reliance of SAA signal transport on vascular connections. Petiole dye feeding revealed that rapid transport through the phloem in Arabidopsis follows the known helical phyllotaxis of 135.5°, where every 3rd clockwise leaf and every 5th counter-clockwise leaf will have strong vascular connections, and also that there is some flow into indirectly connected leaves 1 h after infiltration, as suggested by studies in other plant species (Orians et al., 2000). SAA marker genes were similarly assayed with qPCR (Figs. 8 and 9). The major conclusions of these experiments were that some SAA signals are mostly induced in orthostichous leaves in the immediate response, whereas signaling becomes more uniform between connected and unconnected leaves over time. This later phase of uniform tolerance to photo-oxidative stress was also seen across the rosette after 1 h SAA treatment in a previous study (Gordon et al., 2013).

Refining this generalization, more detailed analysis of each gene revealed distinct differences in expression under HL both spatially and temporally. The activity of two $^1O_2$-specific SAA genes, *RRTF1* and *NodL*, demonstrated conclusively the importance of direct leaf connections. *RRTF1* was significantly induced in orthostichous tissue after 5 min HL; induction then became more uniform across both connected and unconnected leaves by 1 h. *NodL*, in contrast, had a slower HL response proportional to the length of HL exposure and, subsequently, a more delayed SAA-response exclusive to orthostichous tissue. Furthermore, only *NodL*, a $^1O_2$-specific plasma membrane protein, was expressed exclusively in orthostichous distal tissues. This could mean that *NodL* is involved in longer term developmental signaling that could result in differential phenotype development (Coupe et al., 2006; Araya et al., 2008; Gorsuch et al., 2010). In contrast, *ZAT10* induction was variable and only *ZAT10* favored developmental leaf positions over those with direct connections. These differences in gene expression likely emphasize the many different response pathways initiated by HL and SAA. Regardless of leaf connections, 1 h HL treatments in this study resulted in higher induction of *ZAT10* and *RRTF1* in older tissues, whereas LUC expression from the HL-specific *ZAT10* promoter and *NodL* expression favored younger tissues (Figs. 6 and 7). Based on these results, the vascular connection appears to be important for the immediate SAA transcription factor response, which becomes stronger in all older tissues within 1 h of HL stress, whereas longer term SAA signals are directed toward younger tissues and may be required for the development of acclimation phenotypes in new tissues.

High levels of induction are therefore capable of changing source-sink relationships and may result in more general allocation of acclimation resources across the rosette (Arnold and Schultz, 2002; Arnold et al., 2004). A reason younger, and particularly developing, tissues may be more likely to receive signals regardless of orthostichy is that symplastic transport is more likely to occur early in tissue development due to high sieve element number and plasmodesmal (Pd) density, whereas mature sieve elements have very little symplastic exchange (Orians et al., 2005). As a result, adjacent sieve elements, and therefore adjacent leaves, are more likely to receive a signal from the phloem. Arabidopsis is an apoplastic loader, in which Suc produced during photosynthesis in BSC and phloem parenchyma cells, for example, is first exported into the apoplast, actively loaded into the sieve element-companion cell complex, and finally transported via Pd from the companion cell to the sieve element (Lalonde et al., 2004; Zavaliev et al., 2010). Pd have been speculated to be important for cell-to-cell signaling models (Mullineaux and Baker, 2010; Karpinski et al., 2011), and signals such as siRNAs are known to move through these channels from cell-to-cell over a short range and through the phloem over longer distances (Kalantidis et al., 2008).

### A Potentially Volatile SAA Signaling Molecule

An alternative possibility for future SAA research is investigation into the involvement of volatile organic compounds (VOCs), which can overcome the spatial and temporal restrictions of the vascular system (Turnbull, 2011). These have already been shown to be involved in abiotic defense (Heil et al., 2007; Heil and Ton, 2008; Arimura et al., 2011). One possibility for a $^1O_2$-specific and HL-induced SAA volatile molecule is an oxidized form of β-carotene, β-cyclocitral (Ramel et al., 2012). Exogenous application of this molecule is able to induce $^1O_2$-responsive genes and it is thought to be capable of both volatile and vascular transport (Ramel et al., 2012). Oxidative cleavage of carotenoids by $^1O_2$ would occur very early in a HL stress event within the chloroplast. Not only could this molecule be involved at an earlier step in the HL response to the EX1/EX2 retrograde signal, but also externally as a volatile.

As β-cyclocitral has been shown to be independent of EXECUTER-retrograde signaling, this may explain the inability for the localized HL treatment to induce this compound in local HL-stressed tissue (Fig. 10). As $^1O_2$ can also regulate PCD via CRY1 signaling, this might be part of a β-cyclocitral EXECUTER-independent signaling pathway, distinct from SAA (Danon et al., 2006; Ramel et al., 2013). For example, CRY1 regulates chloroplast movement through PHOTOTROPIN1 (PHOT1) and PHOT2, photoprotective anthocyanin accumulation, as well as cell death signaling pathways (Li et al., 2009). CRY1 is also considered crucial to the HL response via ELIPS (Hutin et al., 2003; Kleine et al., 2007; Bechtold et al., 2008). Similarly, results from this current study also support indirect evidence that SAA signals may be independent of downstream CRY1 signaling (Fig. 6), particularly as SAA is EXECUTER-dependent, while CRY1-dependent β-cyclocitral signaling is EXECUTER-independent (Fig. 5).

Different β-carotene oxidation products demonstrate specificity to both acclimation and cell death in the same pathway (Ramel et al., 2012; Shumbe et al., 2014). For example, Lv et al. (2015) have demonstrated a connection between β-cyclocitral and SA during wounding. Interestingly, another HL-induced β-carotene derivative, dihydroactinidiolide, has been shown to be able to induce $^1O_2$-derived photo-acclimation in Arabidopsis and would be an ideal target of future studies into acclimation and even SAA signaling (Shumbe et al., 2014).

VOCs can be produced very rapidly, cover larger areas than vascular signaling, and could solve the problem of stress specificity. Indeed, the uniform spatial distribution of SAA TF transcripts in distal tissue after 1 h of HL exposure can be seen in contrast to transcripts such as *NodL* that may be involved in the longer term developmental signals expressed exclusively in an orthostichous and/or a source-to-sink manner (Fig. 6). However, microarray comparison between SAA and β-cyclocitral transcriptional responses reveals a modest 20% overlap of SAA genes, which are also induced by β-cyclocitral (Fig. 9). The low percentage of genes in common suggests that β-cyclocitral has additional functions other than just SAA. Furthermore, many of these shared genes encode proteins expressed in the chloroplast, nucleus, plasma membrane, and plasmodesmata, together supporting both cell-to-cell and volatile signaling (Supplemental Table S4). While it is likely that VOCs are involved in SAA, no evidence was obtained in this study supporting the involvement of β-cyclocitral; therefore, more severe HL-induced oxidative stress might be required for its induction, but this should be clarified in future work.

### Conclusion

This study further improves our understanding of how environmentally sensed signals can move rapidly through a plant undergoing localized HL stress in order to induce rapid systemic acclimation. Results indicate the importance of $^1O_2$ in initiating the HL-specific systemic response as well as the extracellular involvement of $H_2O_2$ required for transmission of the signal to neighboring and distal unstressed tissues. Furthermore, we have demonstrated that there are different spatial and temporal responses to SAA that reflect multiple processes that may require volatiles and systemic signals, orthostichous connections, developmental stage of the leaves and a temporal component to each process. These new findings alongside other recent publications reveal further possibilities of investigation into SAA with the hypothesis that rapid volatile signals are followed by slower vascular signals through the phloem.

## MATERIALS AND METHODS

### Plant Material and Growth Conditions

For all experiments, Arabidopsis (*Arabidopsis thaliana*; Col-0) and mutants except *flu* were cultivated in soil under a 12 h photoperiod of 150 ± 25 μmol photons $m^{-2}$ $s^{-1}$, 23/22 ± 2°C day/night temperatures, and 70 ± 10% day/night RH. HL treatments were performed with a light emitting diode (LED)-array system, previously detailed in Gordon et al. (2013) using mature (approximately 4 weeks old) Arabidopsis plants at the 12–15 leaf stage. Arabidopsis leaf positions for tissue collection were counted according to Arabidopsis phyllotaxy (Jürgens, 2001). Individual leaves of nine plants were simultaneously exposed to HL (1500 ± 50 μmol photons $m^{-2}$ $s^{-1}$) or to LL conditions (40 ± 25 μmol photons $m^{-2}$ $s^{-1}$). Subsequently, HL (leaf 6), control (leaf 6), and distal tissues (leaf labels and positions: D1, 5; D2, 7; O1, 3; O2; 9) from three treated individual plants were pooled to yield one of three biological replicates per tissue. These were immediately frozen in liquid $N_2$, and stored at −80°C. The chloroplast movement that occurs in tissues directly exposed to 1 h HL (Fig. 6A) serves as a marker for specific collection of directly exposed tissues. HL treatments were performed for 5 min, 30 min, and 1 h durations for qPCR experiments, and longer time courses with 1, 2, 3, 6, and 12 h localized exposure times for HL defense phenotype assays. The conditional *flu* mutant, in the *Landsberg* (*Ler*) background, was grown under continuous light along with *Ler* controls. Stress treatments to induce localized endogenous $^1O_2$ involved covering a single leaf (6) each of *flu* (*Ler*) and *Ler* control plant for 12 h in the dark overnight to allow for accumulation of protochlorophyllide. The leaf covers

were removed for 1 h in growth light, and tissues were sampled as previously described. ZAT10::LUC lines have been described previously in (Rossel et al., 2007). The number of experimental repetitions for each mutant and transgenic background were as follows: wild type, 9; *ex1*, 6; *ex2*, 4; *ex1/2*, 5; *rbohD/F*, 6; *flu*, 3; *Ler*, 3; *tapx*, 3; tAPX-OE, 3.

## Rhodamine B and Aminotriazole Infiltrations

Vasculature was infiltrated with either 2 mM aminotriazole or 0.25% dye via petiole infiltration. Either aminotriazole or rhodamine B dye was infiltrated into plants at various leaf positions through the petiole. The petiole was cut under water to maintain vascular pressure, then submerged in a PCR-sized eppi containing the infiltration solution (Aminotriazole 1.138 g/mol, 10 mL of 2 mM 3-aminotriazole stock solution; 0.25% Rhodamine B). The eppi was stabilized by pressing it into the soil. Plants were moved back to the growth room and leaves were scored for varying degrees of dye infiltration (strong, medium, weak, none) based on leaf position at multiple time points over several days.

## qPCR Analysis

RNA was extracted from frozen samples using an RNeasy Plant Mini Kit (Qiagen, Ltd.) following manufacturer's instructions. RNA was converted to cDNA using SuperScript III Reverse Transcriptase (Invitrogen), and qPCR was performed using a LightCycler 480 (Roche) with either the LightCycler Universal ProbeLibrary or Sybr green specified by the manufacturer's instructions. The LightCycler 480 software application (Roche; version 1.5.0) was used to determine crossing-point values for each reaction, amplification efficiency of each primer set, validation of each reaction, and relative expression values obtained as described in (Pfaffl, 2001). For qPCR and primer validation experiments, the target transcript levels were normalized to two reference genes, *CYCLOPHILIN 5* (*CYP5*) and *PROTEIN PHOSPHATASE 2A* (*PP2A*). A list of primers is outlined in Supplemental Table S3. *ELIP2* induction functioned as a specific marker for successful HL induction in exposed tissues and was assayed in all experiments. Statistical significance of results was tested by conducting paired Student's *t* tests (between LL controls and other samples) and one-way ANOVA on all samples using the statistical analysis program, SigmaPlot12 (Systat Software, Inc.). LSD (LSD) and Holm-Sidak post hoc tests were used where one-way ANOVAs indicated significant differences between factors.

## Microarray Comparison

Microarray data from Rossel et al. (2007) was directly compared to ROS responsive and specific gene sets described in Gadjev et al., (2006). Only gene transcripts that demonstrated significant changes in gene expression were considered in this comparison. Area proportional Venn diagrams were created using BioVenn software (Hulsen et al., 2008). The Genevestigator software was used to determine whether the $^1O_2$ marker, *AAA-ATPase*, was differentially expressed between LL and HL tissues across multiple arrays (Hruz et al., 2008).

## GC/MS Measurements of β-Cyclocitral

GC/MS measurements of β-cyclocitral were performed as described previously (Ramel et al., 2012). Col-0 plant were treated with localized 1500 μmol photons $m^{-2}$ $s^{-1}$ HL. Tissues were pooled from multiple connected and unconnected leaf tissues per plant. β-cyclocitral was extracted in dichloromethane containing 4-nonanol as an internal reference (10 μg/500 μL final volume). After centrifugation, supernatant was collected and evaporated. Analyses were performed by GC-MS as previously described (Ramel et al., 2012).

## Anthocyanin Accumulation Assays

Extraction of anthocyanin pigments was carried out using a method adapted from the following publications (Neff and Chory, 1998; Abdel-Aal and Hucl, 1999; Kong et al., 2003). Briefly, 300 mL of anthocyanin extraction buffer (MeOH, pH 1.0) and a steel ball was added to each sample followed by homogenization in a Tissue Lyser II (Qiagen) at 25 Hz for 90 min. An amount of 250 mL of chloroform and 200 mL of $H_2O$ were added to the homogenate, the samples were briefly mixed by vortexing, and then were centrifuged at 14,000 rpm for 5 min. A total of 200 mL of the upper aqueous phase of each sample was transferred to a 96-well microtitre plate. The determination of total anthocyanins is based on Lambert-Beer's law, where the maximum absorbance (530) will be proportional to the anthocyanin content of the sample; background absorbance was measured at 657 nm. A530 and A657 were determined using a μQuant plate reader (Bio-Tek Instruments) and the Kineticale software (Bio-Tek Instruments; version 3.4). A mixture of 125 mL of chloroform and 100 mL of $H_2O$ was used as a reagent blank.

## Imaging and Scanalyzer Analyses

LUC imaging was performed using a CCD camera to measure luciferin luminescence. The LUC substrate solution: 100 mM luciferin and 1 drop of tween were combined to a total volume of 10 mL. After LUC application of the whole plant, plants were left for 15 min in the dark to increase transpiration and uptake of substrate into leaf tissues. The scanalyzer (www.lemnatec.com) was used to monitor photobleaching development in Col-0 and mutant lines growth under continuous HL for 3 d.

## Accession Numbers

Sequence data from this article can be found in the GenBank/EMBL data libraries under accession numbers ZAT10, At1g27730; RRTF1, At4g34410; NodL, At5g64870; ELIP2, At4g14690; FER1, At5g01600; AAA-ATPase, At3g28580; BAP1, At3g61190; CYP5, At2g29960; PP2A, At1g13320.

## Supplemental Data

The following supplemental materials are available.

**Supplemental Figure S1.** Commonly used ROS marker genes, *FER1* and *AAA-ATPase* are not induced by LED HL in stable silenced and overexpressing tAPX lines.

**Supplemental Figure S2.** Comparison of photobleaching development between ROS signaling mutants.

**Supplemental Figure S3.** Basal *ZAT10* and *RRTF1* induction in LL tissue of wild type and ROS signaling mutants.

**Supplemental Figure S4.** Anthocyanin Assays.

**Supplemental Figure S5.** Rhodamine B infiltrations.

**Supplemental Figure S6.** 5 min and 1h timepoints from the HL spot treatment of ZAT10::LUC HL-specific transgenics.

**Supplemental Table S1.** ROS-responsive SAA gene list. ROS-responsive gene sets obtained from Gadjev et al. (2006) and compared with SAA-specific genes from Rossel et al. (2007).

**Supplemental Table S2 A.** Statistical tests for differences within ZAT10 ROS-signaling mutant data sets.

**Supplemental Table S2 B.** Statistical tests for differences within RRTF1 ROS-signaling mutant data sets.

**Supplemental Table S3.** Statistical analysis results for connected and unconnected leaf data sets.

**Supplemental Table S4.** Shared β-cyclocitral and SAA genes. Shared genes from the β-cyclocitral (Ramel et al., 2012) and SAA (Rossel et al., 2007) microarrays.

**Supplemental Table S5.** qRT-PCR primers and used for Roche (with UPL probes) and SybrGreen for quantitative transcript analysis.

## ACKNOWLEDGMENTS

We would like to thank Dr. Teresa Neeman for statistical advice for the qPCR analyses and Bertrand Légeret (CEA Cadarache) for help with the measurements of β-cyclocitral. We would also like to thank two anonymous reviewers for their invaluable comments and feedback and to the 2014 ANU BIOL3161 undergraduate Honours pathway class for processing, analyzing, and discussing an experimental repeat from the conditional *flu* mutant experiment.

Received March 16, 2016; accepted June 9, 2016; published June 10, 2016.

## LITERATURE CITED


**Abdel-Aal E-SM, Hucl P** (1999) A Rapid Method for Quantifying Total Anthocyanins in Blue Aleurone and Purple Pericarp Wheats. Cereal Chem **76:** 350–354

**Alboresi A, Dall'osto L, Aprile A, Carillo P, Roncaglia E, Cattivelli L, Bassi R** (2011) Reactive oxygen species and transcript analysis upon excess light treatment in wild-type Arabidopsis thaliana vs a photosensitive mutant lacking zeaxanthin and lutein. BMC Plant Biol **11:** 62

**Araya T, Noguchi K, Terashima I** (2008) Manipulation of light and CO2 environments of the primary leaves of bean (Phaseolus vulgaris L.) affects photosynthesis in both the primary and the first trifoliate leaves: involvement of systemic regulation. Plant Cell Environ **31:** 50–61

**Arimura G, Ozawa R, Maffei ME** (2011) Recent advances in plant early signaling in response to herbivory. Int J Mol Sci **12:** 3723–3739

**Arnold T, Appel H, Patel V, Stocum E, Kavalier A, Schultz J** (2004) Carbohydrate translocation determines the phenolic content of Populus foliage: a test of the sink-source model of plant defense. New Phytol **164:** 157–164

**Arnold T, Schultz J** (2002) Induced sink strength as a prerequisite for induced tannin biosynthesis in developing leaves of Populus. Oecologia **130:** 585–593

**Baruah A, Simková K, Apel K, Laloi C** (2009) Arabidopsis mutants reveal multiple singlet oxygen signaling pathways involved in stress response and development. Plant Mol Biol **70:** 547–563

**Bechtold U, Richard O, Zamboni A, Gapper C, Geisler M, Pogson B, Karpinski S, Mullineaux PM** (2008) Impact of chloroplastic- and extracellular-sourced ROS on high light-responsive gene expression in Arabidopsis. J Exp Bot **59:** 121–133

**Carmody M, Pogson BJ** (2013) Systemic photo-oxidative stress signaling. *In* Long-distance systemic signaling and communication in plants, vol. 19, ed. Baluška F, Springer-Verlag Berlin Heidelberg, pp. 251–274

**Chan KX, Phua SY, Crisp P, McQuinn R, Pogson BJ** (2016) Learning the Languages of the Chloroplast: Retrograde Signaling and Beyond. Annu Rev Plant Biol **67:** 25–53

**Cheng H, Zhang Q, Guo D** (2013) Genes that respond to $H_2O_2$ are also evoked under light in Arabidopsis. Mol Plant **6:** 226–228

**Coupe SA, Palmer BG, Lake JA, Overy SA, Oxborough K, Woodward FI, Gray JE, Quick WP** (2006) Systemic signalling of environmental cues in Arabidopsis leaves. J Exp Bot **57:** 329–341

**Danon A, Coll NS, Apel K** (2006) Cryptochrome-1-dependent execution of programmed cell death induced by singlet oxygen in Arabidopsis thaliana. Proc Natl Acad Sci USA **103:** 17036–17041

**Davletova S, Schlauch K, Coutu J, Mittler R** (2005) The zinc-finger protein Zat12 plays a central role in reactive oxygen and abiotic stress signaling in Arabidopsis. Plant Physiol **139:** 847–856

**Esau K** (1953) Plant anatomy. Wiley, New York

**Evert RF, Esau K** (2006) Esau's Plant anatomy: meristems, cells, and tissues of the plant body, 3rd ed. John Wiley and Sons, USA

**Fryer MJ, Ball L, Oxborough K, Karpinski S, Mullineaux PM, Baker NR** (2003) Control of Ascorbate Peroxidase 2 expression by hydrogen peroxide and leaf water status during excess light stress reveals a functional organisation of Arabidopsis leaves. Plant J **33:** 691–705

**Gadjev I, Vanderauwera S, Gechev TS, Laloi C, Minkov IN, Shulaev V, Apel K, Inzé D, Mittler R, Van Breusegem F** (2006) Transcriptomic footprints disclose specificity of reactive oxygen species signaling in Arabidopsis. Plant Physiol **141:** 436–445

**Galvez-Valdivieso G, Fryer MJ, Lawson T, Slattery K, Truman W, Smirnoff N, Asami T, Davies WJ, Jones AM, Baker NR, Mullineaux PM** (2009) The high light response in Arabidopsis involves ABA signaling between vascular and bundle sheath cells. Plant Cell **21:** 2143–2162

**Gilroy S, Suzuki N, Miller G, Choi W-G, Toyota M, Devireddy AR, Mittler R** (2014) A tidal wave of signals: calcium and ROS at the forefront of rapid systemic signaling. Trends Plant Sci **19:** 623–630

**Gilroy S, Białasek M, Suzuki N, Górecka M, Devireddy A, Karpinski S, Mittler R** (2016) ROS, calcium and electric signals: Key mediators of rapid systemic signaling in plants. Plant Physiol **171:** 1606–1615

**Gordon MJ, Carmody M, Albrecht V, Pogson B** (2013) Systemic and local responses to repeated HL stress-induced retrograde signaling in Arabidopsis. Front Plant Sci **3:** 303

**Gorecka M, Alvarez-Fernandez R, Slattery K, McAusland L, Davey PA, Karpinski S, Lawson T, Mullineaux PM** (2014) Abscisic acid signalling determines susceptibility of bundle sheath cells to photoinhibition in high light-exposed Arabidopsis leaves. Philos Trans R Soc Lond B Biol Sci **369:** 20130234

**Gorsuch PA, Sargeant AW, Penfield SD, Quick WP, Atkin OK** (2010) Systemic low temperature signaling in Arabidopsis. Plant Cell Physiol **51:** 1488–1498

**Havaux M** (2014) Carotenoid oxidation products as stress signals in plants. Plant J **79:** 597–606

**Havaux M, Dall'osto L, Bassi R** (2007) Zeaxanthin has enhanced antioxidant capacity with respect to all other xanthophylls in Arabidopsis leaves and functions independent of binding to PSII antennae. Plant Physiol **145:** 1506–1520

**Havaux M, Triantaphylidès C, Genty B** (2006) Autoluminescence imaging: a non-invasive tool for mapping oxidative stress. Trends Plant Sci **11:** 480–484

**Heil M, Silva Bueno JC** (2007) Within-plant signaling by volatiles leads to induction and priming of an indirect plant defense in nature. Proc Natl Acad Sci USA **104:** 5467–5472

**Heil M, Ton J** (2008) Long-distance signalling in plant defence. Trends Plant Sci **13:** 264–272

**Hruz T, Laule O, Szabo G, Wessendorp F, Bleuler S, Oertle L, Widmayer P, Gruissem W, Zimmermann P, Hruz T, Laule O, Szabo G, Wessendorp F, Bleuler S, Oertle L, Widmayer P, Gruissem W, Zimmermann P** (2008) Genevestigator v3: a reference expression database for the meta-analysis of transcriptomes. Adv Bioinforma **2008:** 420747

**Hulsen T, de Vlieg J, Alkema W** (2008) BioVenn - a web application for the comparison and visualization of biological lists using area-proportional Venn diagrams. BMC Genomics **9:** 488

**Hutin C, Nussaume L, Moise N, Moya I, Kloppstech K, Havaux M** (2003) Early light-induced proteins protect Arabidopsis from photooxidative stress. Proc Natl Acad Sci USA **100:** 4921–4926

**Jung H-S, Crisp PA, Estavillo GM, Cole B, Hong F, Mockler TC, Pogson BJ, Chory J** (2013) Subset of heat-shock transcription factors required for the early response of Arabidopsis to excess light. Proc Natl Acad Sci USA **110:** 14474–14479

**Jürgens G** (2001) Apical-basal pattern formation in Arabidopsis embryogenesis. EMBO J **20:** 3609–3616

**Kalantidis K, Schumacher HT, Alexiadis T, Helm JM** (2008) RNA silencing movement in plants. Biol Cell **100:** 13–26

**Kangasjärvi S, Lepistö A, Hännikäinen K, Piippo M, Luomala EM, Aro EM, Rintamäki E** (2008) Diverse roles for chloroplast stromal and thylakoid-bound ascorbate peroxidases in plant stress responses. Biochem J **412:** 275–285

**Karpinski S, Van Breusegem F, Karpinska B, Kornas A, Szechynska-Hebda M, Vanderauwera S, Slesak I, Wituszynska W** (2011) The algorithmic regulation of Darwinian fitness traits in plants. Soc. Exp. Biol. Annu. Main Meet.

**Karpinski S, Reynolds H, Karpinska B, Wingsle G, Creissen G, Mullineaux P** (1999) Systemic signaling and acclimation in response to excess excitation energy in Arabidopsis. Science **284:** 654–657

**Karpiński S, Szechyńska-Hebda M** (2010) Secret life of plants: from memory to intelligence. Plant Signal Behav **5:** 1391–1394

**Kiefer IW, Slusarenko AJ** (2003) The pattern of systemic acquired resistance induction within the Arabidopsis rosette in relation to the pattern of translocation. Plant Physiol **132:** 840–847

**Kim C, Meskauskiene R, Zhang S, Lee KP, Lakshmanan Ashok M, Blajecka K, Herrfurth C, Feussner I, Apel K** (2012) Chloroplasts of Arabidopsis are the source and a primary target of a plant-specific programmed cell death signaling pathway. Plant Cell **24:** 3026–3039

**Kim C, Meskauskiene R, Apel K, Laloi C** (2008) No single way to understand singlet oxygen signalling in plants. EMBO Rep **9:** 435–439

**Kleine T, Kindgren P, Benedict C, Hendrickson L, Strand A** (2007) Genome-wide gene expression analysis reveals a critical role for CRYPTOCHROME1 in the response of Arabidopsis to high irradiance. Plant Physiol **144:** 1391–1406

**Kong J-M, Chia L-S, Goh N-K, Chia T-F, Brouillard R** (2003) Analysis and biological activities of anthocyanins. Phytochemistry **64:** 923–933

**Kwak JM, Mori IC, Pei Z-M, Leonhardt N, Torres MA, Dangl JL, Bloom RE, Bodde S, Jones JDG, Schroeder JI** (2003) NADPH oxidase AtrbohD and AtrbohF genes function in ROS-dependent ABA signaling in Arabidopsis. EMBO J **22:** 2623–2633

**Laloi C, Havaux M** (2015) Key players of singlet oxygen-induced cell death in plants. Front Plant Sci **6:** 39

**Laloi C, Stachowiak M, Pers-Kamczyc E, Warzych E, Murgia I, Apel K** (2007) Cross-talk between singlet oxygen- and hydrogen peroxide-dependent signaling of stress responses in Arabidopsis thaliana. Proc Natl Acad Sci USA **104:** 672–677

**Lalonde S, Wipf D, Frommer WB** (2004) Transport mechanisms for organic forms of carbon and nitrogen between source and sink. Annu Rev Plant Biol **55:** 341–372

**Lee KP, Kim C, Landgraf F, Apel K** (2007) EXECUTER1- and EXECUTER2-dependent transfer of stress-related signals from the plastid to the nucleus of Arabidopsis thaliana. Proc Natl Acad Sci USA **104:** 10270–10275

**Li Z, Wakao S, Fischer BB, Niyogi KK** (2009) Sensing and responding to excess light. Annu Rev Plant Biol **60:** 239–260

**Lv F, Zhou J, Zeng L, Xing D** (2015) $\beta$-cyclocitral upregulates salicylic acid signalling to enhance excess light acclimation in Arabidopsis. J Exp Bot **66:** 4719–4732

**Maruta T, Tanouchi A, Tamoi M, Yabuta Y, Yoshimura K, Ishikawa T, Shigeoka S** (2010) Arabidopsis chloroplastic ascorbate peroxidase isoenzymes play a dual role in photoprotection and gene regulation under photooxidative stress. Plant Cell Physiol **51:** 190–200

**Maruta T, Noshi M, Tanouchi A, Tamoi M, Yabuta Y, Yoshimura K, Ishikawa T, Shigeoka S** (2012) H2O2-triggered retrograde signaling from chloroplasts to nucleus plays specific role in response to stress. J Biol Chem **287:** 11717–11729

**Meskauskiene R, Nater M, Goslings D, Kessler F, op den Camp R, Apel K** (2001) FLU: a negative regulator of chlorophyll biosynthesis in Arabidopsis thaliana. Proc Natl Acad Sci USA **98:** 12826–12831

**Miller G, Schlauch K, Tam R, Cortes D, Torres MA, Shulaev V, Dangl JL, Mittler R** (2009) The plant NADPH oxidase RBOHD mediates rapid systemic signaling in response to diverse stimuli. Sci Signal **2:** ra45

**Mittler R, Blumwald E** (2015) The Roles of ROS and ABA in Systemic Acquired Acclimation. Plant Cell tpc.114.133090–

**Mittler R, Vanderauwera S, Gollery M, Van Breusegem F** (2004) Reactive oxygen gene network of plants. Trends Plant Sci **9:** 490–498

**Mittler R, Vanderauwera S, Suzuki N, Miller G, Tognetti VB, Vandepoele K, Gollery M, Shulaev V, Van Breusegem F** (2011) ROS signaling: the new wave? Trends Plant Sci **16:** 300–309

**Mullineaux PM, Baker NR** (2010) Oxidative stress: antagonistic signaling for acclimation or cell death? Plant Physiol **154:** 521–525

**Murgia I, Tarantino D, Vannini C, Bracale M, Carravieri S, Soave C** (2004) Arabidopsis thaliana plants overexpressing thylakoidal ascorbate peroxidase show increased resistance to Paraquat-induced photooxidative stress and to nitric oxide-induced cell death. Plant J **38:** 940–953

**Neff MM, Chory J** (1998) Genetic interactions between phytochrome A, phytochrome B, and cryptochrome 1 during Arabidopsis development. Plant Physiol **118:** 27–35

**Oelze M-L, Vogel MO, Alsharafa K, Kahmann U, Viehhauser A, Maurino VG, Dietz K-J** (2012) Efficient acclimation of the chloroplast antioxidant defence of Arabidopsis thaliana leaves in response to a 10- or 100-fold light increment and the possible involvement of retrograde signals. J Exp Bot **63:** 1297–1313

**op den Camp RGL, Przybyla D, Ochsenbein C, Laloi C, Kim C, Danon A, Wagner D, Hideg E, Göbel C, Feussner I, et al** (2003) Rapid induction of distinct stress responses after the release of singlet oxygen in Arabidopsis. Plant Cell **15:** 2320–2332

**Orians C** (2005) Herbivores, vascular pathways, and systemic induction: facts and artifacts. J Chem Ecol **31:** 2231–2242

**Orians CM, Pomerleau J, Ricco R** (2000) Vascular architecture generates fine scale variation in systemic induction of proteinase inhibitors in tomato. J Chem Ecol **26:** 471–485

**Orians CM, Smith SDP, Sack L** (2005) How are leaves plumbed inside a branch? Differences in leaf-to-leaf hydraulic sectoriality among six temperate tree species. J Exp Bot **56:** 2267–2273

**Pfaffl MW** (2001) A new mathematical model for relative quantification in real-time RT-PCR. Nucleic Acids Res **29:** e45

**Przybyla D, Göbel C, Imboden A, Hamberg M, Feussner I, Apel K** (2008) Enzymatic, but not non-enzymatic, 1O2-mediated peroxidation of polyunsaturated fatty acids forms part of the EXECUTER1-dependent stress response program in the flu mutant of Arabidopsis thaliana. Plant J **54:** 236–248

**Ramel F, Birtic S, Ginies C, Soubigou-Taconnat L, Triantaphylidès C, Havaux M** (2012) Carotenoid oxidation products are stress signals that mediate gene responses to singlet oxygen in plants. Proc Natl Acad Sci USA **109:** 5535–5540

**Ramel F, Ksas B, Akkari E, Mialoundama AS, Monnet F, Krieger-Liszkay A, Ravanat J-L, Mueller MJ, Bouvier F, Havaux M** (2013) Light-induced acclimation of the Arabidopsis chlorina1 mutant to singlet oxygen. Plant Cell **25:** 1445–1462

**Rizhsky L, Liang H, Mittler R** (2003) The water-water cycle is essential for chloroplast protection in the absence of stress. J Biol Chem **278:** 38921–38925

**Rossel JB, Wilson PB, Hussain D, Woo NS, Gordon MJ, Mewett OP, Howell KA, Whelan J, Kazan K, Pogson BJ** (2007) Systemic and intracellular responses to photooxidative stress in Arabidopsis. Plant Cell **19:** 4091–4110

**Shao N, Duan GY, Bock R** (2013) A mediator of singlet oxygen responses in Chlamydomonas reinhardtii and Arabidopsis identified by a luciferase-based genetic screen in algal cells. Plant Cell **25:** 4209–4226

**Shen W, Chen G, Xu J, Zhen X, Ma J, Zhang X, Lv C, Gao Z** (2015) High light acclimation of Oryza sativa L. leaves involves specific photosynthetic-sourced changes of NADPH/NADP$^+$ in the midvein. Protoplasma **252:** 77–87

**Shumbe L, Bott R, Havaux M** (2014) Dihydroactinidiolide, a high light-induced $\beta$-carotene derivative that can regulate gene expression and photoacclimation in Arabidopsis. Mol Plant **7:** 1248–1251

**Shumbe L, Chevalier A, Legeret B, Taconnat L, Monnet F, Havaux M** (2016) Singlet Oxygen-Induced Cell Death in Arabidopsis under High-Light Stress Is Controlled by OXI1 Kinase. Plant Physiol **170:** 1757–1771

**Suzuki N, Miller G, Salazar C, Mondal HA, Shulaev E, Cortes DF, Shuman JL, Luo X, Shah J, Schlauch K, Shulaev V, Mittler R** (2013) Temporal-spatial interaction between reactive oxygen species and abscisic acid regulates rapid systemic acclimation in plants. Plant Cell **25:** 3553–3569

**Triantaphylidès C, Krischke M, Hoeberichts FA, Ksas B, Gresser G, Havaux M, Van Breusegem F, Mueller MJ** (2008) Singlet oxygen is the major reactive oxygen species involved in photooxidative damage to plants. Plant Physiol **148:** 960–968

**Turnbull C** (2011) Long-distance regulation of flowering time. J Exp Bot **62:** 4399–4413

**Vanderauwera S, Zimmermann P, Rombauts S, Vandenabeele S, Langebartels C, Gruissem W, Inzé D, Van Breusegem F** (2005) Genome-wide analysis of hydrogen peroxide-regulated gene expression in Arabidopsis reveals a high light-induced transcriptional cluster involved in anthocyanin biosynthesis. Plant Physiol **139:** 806–821

**Viswanathan DV, Thaler JS** (2004) Plant vascular architecture and within-plant spatial patterns in resource quality following herbivory. J Chem Ecol **30:** 531–543

**Wagner D, Przybyla D, Op den Camp R, Kim C, Landgraf F, Lee KP, Würsch M, Laloi C, Nater M, Hideg E, Apel K** (2004) The genetic basis of singlet oxygen-induced stress responses of Arabidopsis thaliana. Science **306:** 1183–1185

**Xia X-J, Zhou Y-H, Shi K, Zhou J, Foyer CH, Yu J-Q** (2015) Interplay between reactive oxygen species and hormones in the control of plant development and stress tolerance. J Exp Bot **66:** 2839–2856

**Yao N, Greenberg JT** (2006) Arabidopsis ACCELERATED CELL DEATH2 modulates programmed cell death. Plant Cell **18:** 397–411

**Zavaliev R, Sagi G, Gera A, Epel BL** (2010) The constitutive expression of Arabidopsis plasmodesmal-associated class 1 reversibly glycosylated polypeptide impairs plant development and virus spread. J Exp Bot **61:** 131–142

**Zhang S, Apel K, Kim C** (2014) Singlet oxygen-mediated and EXECUTER-dependent signalling and acclimation of Arabidopsis thaliana exposed to light stress. Philos Trans R Soc Lond B Biol Sci **369:** 20130227